

VISCOUS AND RHEOLOGIC SUPERPLASTIC TECHNIQUE ^①

He Yuehui, Huang Baiyun and Liu Yong

Powder Metallurgy Research Institute,

Central South University of Technology, Changsha 410083, P. R. China

ABSTRACT A new viscous-rheologic superplastic technique for TiAl based alloy has been explored successfully, which can be divided into three stages: accelerated deformation at large load, viscous-rheologic deformation at low load and final deformation at increasing load. In above three stages, three respective deformation mechanisms exist: coerced grain boundary movement, grain boundary viscous-rheologic sliding, grain boundary sliding aided by sliding inside grains. The damage of recrystallization and neck shrinkage on superplasticity can be avoided in this technique.

Key words TiAl based alloy superplasticity deformation mechanism

1 INTRODUCTION

The application of TiAl based alloy has been hindered by a key problem— its difficulty in cold and hot work, but through proper thermomechanical treatment, excellent room temperature mechanical properties can be obtained in cast TiAl based alloy^[1], which can meet certain serving conditions. Therefore, investigation of near net shaping of hot worked TiAl based alloy helps to accelerate its engineering application. Superplastic shaping is an effective near net shape technique for TiAl based alloy. Generally, study of superplasticity is restricted under the conditions of constant stress^[2] or constant strain^[3]. However, the plasticity of material will be affected by its previous deformation; on the other hand, the deformation behavior of material is not only inherently related to its composition, but also a function of serving conditions. Therefore, at constant strain rate, large plastic deformation can be obtained at certain time, but the strain rate may be relatively low and there is probably potential deformation, which can not be fully realized; on the other hand, the strain rate may also be relatively high because the material needs reparation after large deformation, hence the strain rate should be slowed down.

Therefore, a technique based on above thought and controlling strain rate and stress rate at proper deformation stage will fully exhibit the material's deformability. In addition, the bonding of grain boundaries in TiAl based alloy is so intense that it is difficult for the grains to rotate or slide in hot work, so TiAl based alloy exhibits low thermal deformability. To improve the sessile ability of grain boundaries is a key to obtain large deformation. In this article, viscous deformation and rheologic deformation are adopted to fully exhibit the potential deformability of TiAl based alloy, so as to obtain high strain.

2 EXPERIMENTAL

The nominal composition of the alloy was Ti-33Al-3Cr-0.5Mo(%, in mass), which was smelted in self-consumed arc furnace for two times. The ingot was then homogenization annealed in vacuum at 1 040 °C for 60 h. After HIPped at 1 250 °C, 180 MPa for 6 h, the ingot was canned and experienced multi-step thermomechanical treatment^[4, 5]. Fine, homogeneous duplex microstructure can be obtained in the whole wrought. Plate sample with effective dimension of 2 mm × 3 mm × 12 mm was spark machined from the wrought. Elevated temperature

① Project 715- 005- 0040 supported by National Advanced Materials Committee and National Natural Science Foundation of China

Received Sep. 9, 1996; accepted Nov. 4, 1997

tensile test was conducted in static air with self-made rheologic tensile machine, which can randomly change load and control tensile stress and strain rate. Testing temperature was $970\text{ }^{\circ}\text{C} \pm 10\text{ }^{\circ}\text{C}$. The transverse section of tested sample underwent micrograph observation by using Leica Quantimet optical microscope and X650 scanning electronic microscope.

3 RESULTS

Fig. 1 shows the original duplex microstructure after thermomechanical treatment, the mean grain size is $35\text{ }\mu\text{m}$. The microstructure seems homogeneous. The sample then experienced superplastic deformation. Fig. 2 shows the controlled load-time process curve, and Fig. 3 shows the strain-time relationship curve in respect to Fig. 2. During this process, a final elongation of 194% was obtained and the thermal deformation occurred homogeneously on the ef-

fective length of the tested sample, no apparent neck shrinkage occurred. Based on this result and Fig. 2, the true stress-time relationship curve was drawn in Fig. 4. According to Fig. 2 and Fig. 4, the tensile process can be divided into three stages. The first stage can be described as high load enhanced deformation, in which the maximum true stress was as high as 240 MPa

Fig. 1 Optical micrograph of original microstructure

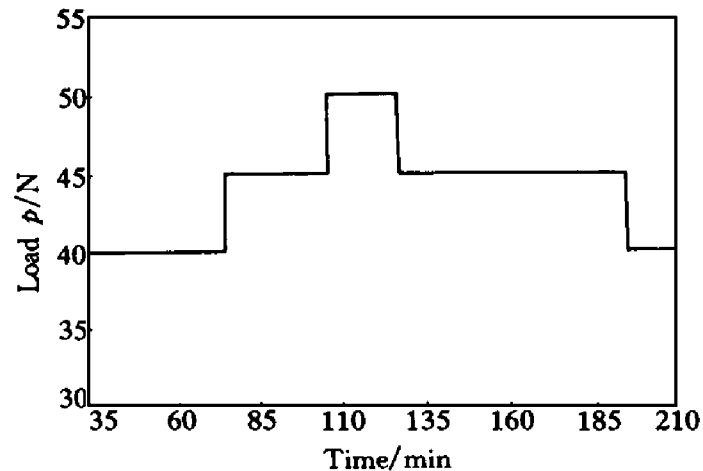
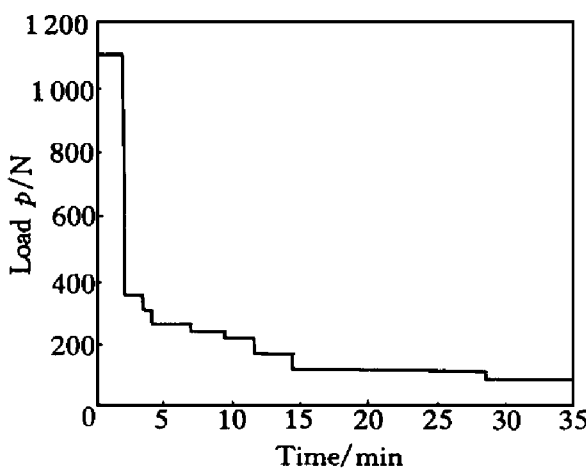


Fig. 2 Process curves of load vs time

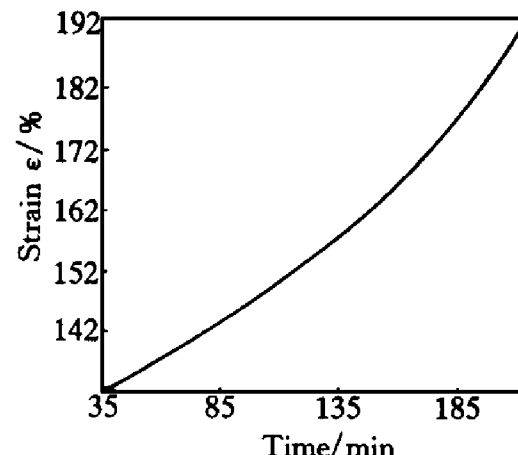
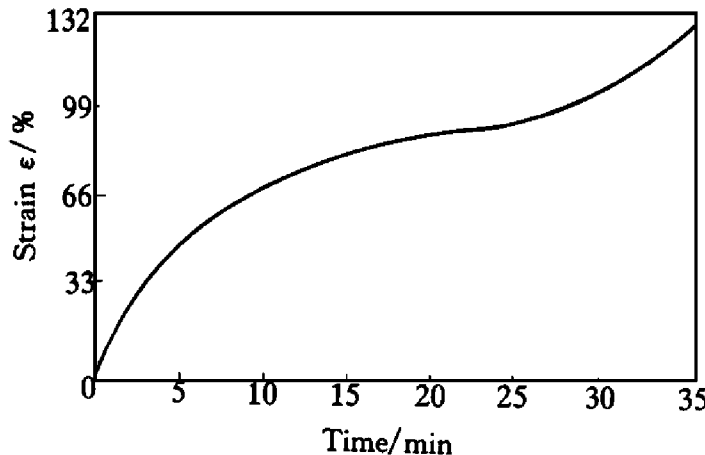
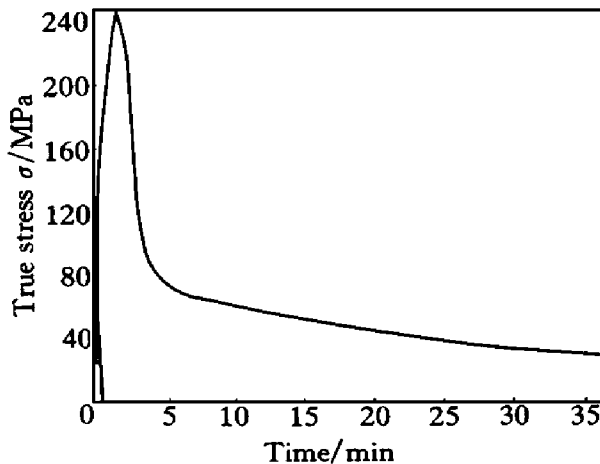


Fig. 3 Strain-time relationship during process of Fig. 2

and an elongation of 33% was completed in 2 minutes with a mean strain rate of $2.9 \times 10^{-3} \text{ s}^{-1}$. Subsequently, the load was decreased to a large extent immediately, and the true stress was just 80 MPa. Then the stress continued to decrease according to variation of strain rate, so as to ensure stable rheologic deformation of the second stage, which can be called low stress viscous and rheologic deformation stage. In this stage, an elongation of 100% was obtained with a mean strain rate of $5.5 \times 10^{-4} \text{ s}^{-1}$. The third stage can be described as increasing load deformation. In the last period of the second stage, at low stress further strain could not be maintained, so the stress had to be increased. In the third stage, the stress increased from 16 MPa to 22 MPa and an elongation of 61% was obtained with a mean strain rate of $3.5 \times 10^{-3} \text{ s}^{-1}$.

After an elongation of 194%, the tested



sample was fractured. The fracture area had regular dimension, no neck shrinkage could be seen. Fig. 5(a) shows the microstructure near the attachment; Fig. 5(b) shows the microstructure near the fracture surface, and Fig. 5(c) shows the microstructures between the above two places. The above three microstructures are almost similar to the original microstructure except that pores exist in Fig. 5(b) and Fig. 5(c). SEM analyses had shown that, pores always exist at the triple points near γ grains and α_2/γ lamellar colony boundaries, but several pores exist inside grains.

4 DISCUSSION

In this work, a high elongation of 194% was obtained in duplex TiAl based alloy under simple test condition. According to deformation

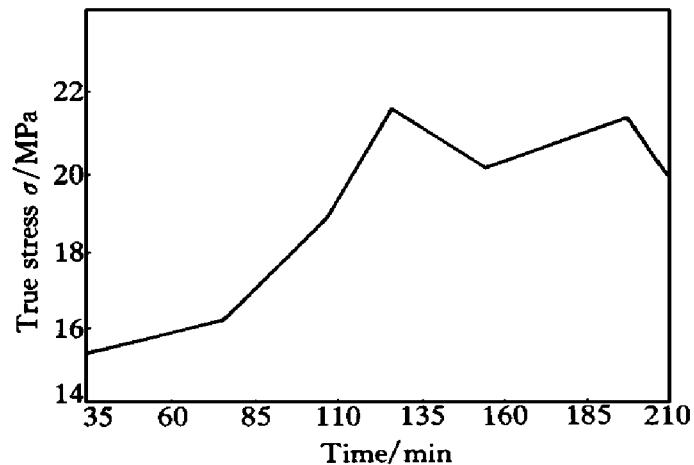


Fig. 4 True stress-time relationship during process of Fig. 2

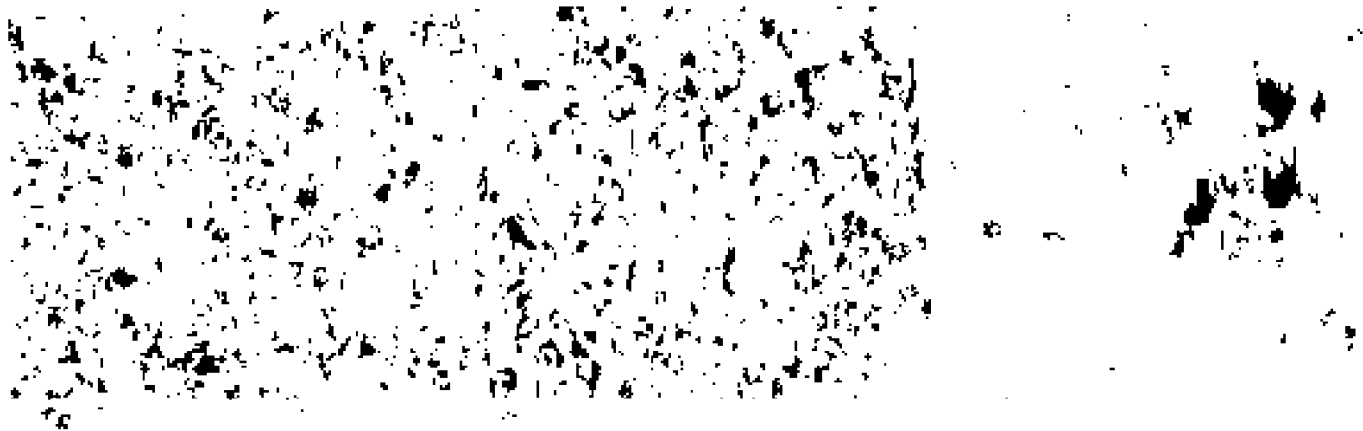


Fig. 5 Optical micrograph of TiAl based alloy after superplastic deformation

(a) —Near the attachment; (b) —Near the fracture surface; (c) —Between (a) and (b)

characteristic, the superplastic process can also be divided into three stages. The first stage is induced deformation at high load and high strain rate. During this stage, the whole deformation proceeded at high stress. At this temperature and strain rate, the yield strength $\sigma_{0.2} = 200$ MPa. TiAl based alloy had ragged grain boundaries and high grain boundary strength, the amorphous thickness was almost nonexistent. At large load, rapid plastic deformation was mainly accomplished through grain boundary sliding and grain rotating. At high stress, the grain boundaries were torn, and flux-like amorphous boundaries were formed. The subsequent grain boundary sliding and grain rotating could be carried on at low stress, so the deformation came into the second stage – viscous-rheologic deformation. In this stage, low strain rate induced slow plastic deformation helped to ensure the reparation of material through heat activated diffusion. This would prevent local area from forming fine recrystallized grains and decreasing strength, which would lead the material to fracture due to stress concentration. When the material had viscous deformability, the flux grain boundaries were thinned due to thermal reparation in deformation, and the material deformation was sped up. In this stage, grain boundary deformation was also the main mechanism, but sliding inside grains began at the same time. The material finally fractured until its deformability was used up. Many pores existed in the fracture surface, they were mainly distributed on grain boundaries and triple points, while some of them existed inside grains. No apparent neck shrinkage was found, which showed that stress concentration due to recrystallization was not the main cause. The fracture mechanism lies in that excessive or inconsistent grain boundary sliding induced the formation of pores which could not be repaired during deformation, therefore led to the increase of true stress and fracture of material from local area of high porosity. The nucleation

and growth of pores are inherent defects in tensile deformation of TiAl based alloy at high temperature, which are mainly accomplished by sliding of grain boundaries due to the difficulty of sliding inside grains. However, once the sliding of TiAl grain boundaries can not continue, pores will form. Therefore, in this work, the plastic deformability of TiAl based alloy has been fully exhibited.

5 CONCLUSIONS

(1) A new viscous-rheologic superplastic technique for TiAl based alloy has been explored successfully, and an elongation of 194% has been obtained.

(2) The new process can be divided into three stages: enhanced deformation at high load, viscous-rheologic deformation at low load and final deformation at increasing load.

(3) In above three stages, three respective deformation mechanisms exist: coerced grain boundary movement, grain boundary viscous-rheologic sliding, grain boundary sliding aided by sliding inside grains.

(4) In this process, the damage of recrystallization and neck shrinkage can be avoided.

(5) The nucleation and growth of pores are the main cause restricting the superplastic deformation of TiAl based alloy.

REFERENCES

- 1 Koepee C *et al.* Metall Trans, 1992, 26: 219.
- 2 He Jinsu, Wang Yanwen. Superplasticity of Metals, (in Chinese). Beijing: Science Press, 1986: 15.
- 3 Edington J W. Metal Tech, 1976, 3: 138.
- 4 He Yuehui *et al.* Hot Working, (in Chinese), 1995, 5: 17.
- 5 He Yuehui *et al.* Mater Sci & Eng, (in Chinese), 1996, 14(1): 35.
- 6 He Yuehui *et al.* Hot Working, (in Chinese), 1996, 4: 7.

(Edited by Yuan Saiqian)